

Class Unbiasing for Generalization in Medical Diagnosis

Lishi Zuo, Man-Wai Mak, Lu Yi, and Youzhi Tu

Abstract

Medical diagnosis might fail due to bias. In this work, we identified class-feature bias, which refers to models' potential reliance on features that are strongly correlated with only a subset of classes, leading to biased performance and poor generalization on other classes. We aim to train a class-unbiased model (Cls-unbias) that mitigates both class imbalance and class-feature bias simultaneously. Specifically, we propose a class-wise inequality loss which promotes equal contributions of classification loss from positive-class and negative-class samples. We propose to optimize a class-wise group distributionally robust optimization objective—a class-weighted training objective that upweights underperforming classes—to enhance the effectiveness of the inequality loss under class imbalance. Through synthetic and real-world datasets, we empirically demonstrate that class-feature bias can negatively impact model performance. Our proposed method effectively mitigates both class-feature bias and class imbalance, thereby improving the model's generalization ability.

Keywords: Class-feature bias, Class imbalance, Medical Diagnosis, Generalization

1 Introduction

Medical data sets are often biased, which compromises the accuracy and reliability of models trained using empirical risk minimization (ERM). A common bias is class imbalance, where models tend to prioritize the majority class at the expense of the minority classes, leading to poor performance on the latter. To mitigate this issue, researchers have proposed various methods, such as oversampling or undersampling classes [1, 2], or using class weights to adjust the loss function [1, 3, 4]. Apart from the class imbalance mentioned in Section 1, there are other invisible biases that arise from spurious features, including patient-specific characteristics (e.g., age [7], gender [7, 8], or speaker identity [3]) and environment-specific factors (e.g., equipment types [7], equipment manufacturers [7], or variations of diagnosis equipment across hospitals [9]). To address these issues, researchers recommend using balanced and diverse training sets and reducing the influence of spurious features in model predictions [8, 3, 7].

However, a critical oversight in current classification methods is the models' potential reliance on features that are strongly correlated with only a subset of classes, leading to biased performance and poor generalization on other classes. Even worse, if such learned correlations are spurious, i.e., correlated by chance rather than causality, the performance on the test set can be catastrophically poor. For example, a model trained on a dataset comprising various biomedical measures of diabetic patients and healthy controls may mistakenly use the body mass index (BMI) to diagnose diabetes. While BMI is strongly correlated with the health conditions that cause diabetes, it is not a good indicator (biomarker) for diagnosing diabetes because people with high BMI may not necessarily have diabetes. Specifically, diabetic patients often have a high BMI, i.e., $P(H | D) > P(L | D)$, where H and L denote high and low BMI, respectively, and D indicates the presence of diabetes. However, this relationship between $P(H|D)$ and $P(L|D)$ is not necessarily true. Instead, it depends on a number of factors, including the population's health conditions and the demography of the subjects in the dataset. As a result, all scenarios— $P(H | D) > P(L | D)$, $P(H | D) < P(L | D)$, or $P(H | D) = P(L | D)$ —are theoretically possible. Therefore, a classifier that relies heavily on the BMI to make decisions has a high chance of classifying non-diabetic samples as diabetic. This phenomenon can be particularly problematic when dealing with imbalanced datasets or complex feature spaces. We define this issue as **class-feature bias**. Generally, class-feature bias refers to models' reliance on features that are correlated with only a subset of classes, leading to biased performance and poor generalization on other classes. In this paper, we focus on mitigating it in binary classification for medical diagnosis, where models tend to prioritize **class-specific features** that are informative for individual classes. Our goal is to develop **class-feature unbiased** models that leverage discriminative features shared across all classes (**class-shared features**).

Notably, the existence of class-feature bias is a major issue in medical diagnosis, where the primary procedure lies in identifying the presence or absence of specific biomarkers or their measured values that distinguish

Lishi ZUO, Man-Wai MAK, Lu YI, and Youzhi TU are with the Department of Electrical and Electronic Engineering, The Hong Kong Polytechnic University, Hong Kong SAR (email: lishi.zuo@connect.polyu.hk, enmwamak@polyu.edu.hk, loulouisa.yi@connect.polyu.hk, 918tyz@gmail.com).

between disease and non-disease states. Therefore, leveraging class-shared features that are informative to both disease and non-disease states can help increase diagnosis accuracy and understand disease mechanisms. Conversely, neglecting these shared features risks overlooking critical indicators of disease progression or response to treatment, potentially leading to misdiagnosis, delayed treatment, or inadequate monitoring. In addition, class-feature bias can be even more problematic under class imbalance scenarios, where one class dominates the dataset, further exacerbating the issue of biased performance. Therefore, developing models that can effectively learn and leverage class-shared features is essential for improving the accuracy and effectiveness of medical diagnoses.

Leveraging insights from information theory, the key intuition to mitigate the class-feature bias is to ensure the features learned by the model are informative for both classes. Specifically, the target-related information in the features for each class can be measured by class-wise cross-entropy classification losses (\mathcal{L}^c and \mathcal{L}^{-c}). Therefore, a **class loss inequality** ($\mathcal{L}^c \neq \mathcal{L}^{-c}$) indicates that the model relies on features that are non-informative to both classes, which can be a sign of existence of class-feature bias under class-balance. Meanwhile, class loss inequality can be also caused by class-imbalance, where the model may under-utilize information from features for the minority class, leading to lower class-wise classification loss. Motivated by [24], we propose a class-wise inequality loss $\mathcal{L}_{\text{cls-ineq}}$ that equalizes the classification losses contributed by the samples from the positive and negative classes, respectively. The class-wise inequality loss can help learn a **class-unbiased model (Cls-unbias)** that mitigates both class imbalance and class-feature bias simultaneously. To improve the effectiveness of the class-wise inequality loss under class imbalance, we combine the cross-entropy loss with a class-wise group distributionally robust optimization (G-DRO) objective [5], which adaptively upweights the high-loss class.

To the authors' best knowledge, this study is the first to identify and treat the class-feature bias as a research problem in deep-learning based medical diagnosis, empirically demonstrating its detrimental effect on binary classification performance. We provide both theoretical and empirical evidence showing the effectiveness of the class-wise inequality loss in addressing class-feature biases in balanced and imbalanced datasets. Extensive experiments were conducted on synthetic and real-world datasets. Our results demonstrate that promoting class-unbiased classification consistently improves model performance across diverse tasks and datasets with different input modalities.

2 Results

2.1 Toy Experiment: Demonstrating and Mitigating the Class-feature Bias

We designed simple experiments using linear classifiers to demonstrate class-feature bias in binary classification under both class-balanced and class-imbalanced conditions. In this section, we illustrated an example of class-specific and class-shared features, and showed that both class imbalance and class-feature bias can negatively impact classification performance of typical ERM (trained using cross-entropy loss only), and that making the classifier unbiased can improve generalization to out-of-distribution scenarios.

Consider a 2D space containing feature vectors \mathbf{x} 's, where $\mathbf{x} = [f_1, f_2]^\top$ is an input feature vector containing two features f_1 and f_2 , and $y \in \{0, 1\}$ is the classification label of \mathbf{x} . We set $f_1 \in \{a, b\}$ and $f_2 \in \{a, b\}$, where $a \sim \mathcal{N}(0, 1)$ and $b \sim \mathcal{N}(3, 1)$. Therefore, we may express $\mathbf{x} = [(a|b), (a|b)]^\top$, where $(a|b)$ means selecting either a or b from the set $\{a, b\}$. We applied this principle to generate three datasets, namely \mathcal{D}^{tr} , $\mathcal{D}^{\text{test1}}$, and $\mathcal{D}^{\text{test2}}$. We used \mathcal{D}^{tr} to train a linear classifier and tested it on $\mathcal{D}^{\text{test1}}$ and $\mathcal{D}^{\text{test2}}$. Fig. 1 and Fig. 2 show the probability distributions of features f_1 and f_2 for the positive class ($y = 1$) and negative class ($y = 0$) under class-balanced and class-imbalanced scenarios, respectively.

Class-shared Feature. In Fig. 1, f_1 is equally effective in classifying \mathbf{x} 's into the positive or negative classes for all datasets (\mathcal{D}^{tr} , $\mathcal{D}^{\text{test1}}$, and $\mathcal{D}^{\text{test2}}$), meaning that it is invariant to the differences in three datasets. Also, f_1 is an example of class-shared features mentioned in Section 1, because it can differentiate both the positive and negative classes.

Class-specific Feature. Fig. 1(a) shows that f_2 is a class-specific feature in \mathcal{D}^{tr} . More specifically, for a classifier that uses f_2 as the only feature, an unknown sample having $f_2 \ll 3$ (say $f_2 = -2$) indicates that it is likely a sample from the positive class (red). Meanwhile, assigning samples with $f_2 \approx 3$ to the negative class (blue) can ensure that all negative samples are correctly classified. Therefore, f_2 is specific to the negative class. On the other hand, Fig. 1(b) and Fig. 1(c) show that f_2 is an irrelevant feature in $\mathcal{D}^{\text{test1}}$ and $\mathcal{D}^{\text{test2}}$, as its value does not determine the class of any unknown samples in these datasets.

Spurious Feature. Applying the model trained in \mathcal{D}^{tr} to the data in $\mathcal{D}^{\text{test2}}$ reveals that f_2 is a spurious feature. This is because although f_2 can partly determine the class labels in the samples in \mathcal{D}^{tr} , it fails to do the same in $\mathcal{D}^{\text{test2}}$.

In the ideal class-unbiased condition, the classifier should learn a vertical decision boundary in Fig. 1 and Fig. 2 to separate the two classes. This means that the classifier pays full attention to f_1 , while assigning no attention to f_2 , resulting in high accuracy on both $\mathcal{D}^{\text{test1}}$ and $\mathcal{D}^{\text{test2}}$. However, the actual decision boundaries

of the linear classifier trained by the ERM (Eq. 1) and the proposed class-unbiased method (Eq. 9) on balanced and imbalanced datasets are shown in Fig. 1 and Fig. 2, respectively. This discrepancy between the ideal and actual decision boundaries suggests the existence of class-specific features and spurious features.

Table 1 shows the classification performance of the linear classifier on the three datasets shown in Fig. 1 and Fig. 2 under class-balanced and class-imbalanced scenarios, respectively. We report the accuracy for the positive and negative classes separately (referred to as pos-acc and neg-acc, respectively) to assess class-wise performance. The classifier comprises two input nodes and one output node, with the normalized weights of the two input features indicated in the last column.¹ To simulate the class-imbalanced and class-balanced situations, we set $p(y = 1) = 0.1$ in the class-imbalanced experiments (Rows 3 and 4) and $p(y = 1) = 0.5$ in the class-balanced experiments (Rows 1 and 2) in the training set. Meanwhile, we kept $p(y = 1) = p(y = 0) = 0.5$ in the test sets for all experiments.

The key conclusions from the toy experiment are summarized below:

1. The classifier trained by ERM (Row 1) relies heavily on the class-specific feature (f_2), as evidenced by the relatively large weights assigned to it. This reliance leads to degraded performance on $\mathcal{D}^{\text{test1}}$ for the positive class. The performance degradation becomes more severe under the class-imbalanced condition, as evident in Row 3. Worse, as mentioned earlier, because f_2 is a spurious feature for $\mathcal{D}^{\text{test2}}$, its performance on the biased class (negative class) can be significantly compromised (Row 1).
2. By comparing the weights in Row 3 with those in Row 1, we observe that class imbalance increases the model’s reliance on the unintended feature f_2 . This leads to improved detection of the negative samples but significantly degrades the performance on the positive samples. The model in Row 3 exhibits the combined effects of class-specific bias and class imbalance, which jointly distort the learned decision boundaries and amplify the asymmetric performance between the two classes.
3. In all situations, Cls-unbias, which promotes the reduction of class loss inequality, can effectively alleviate the reliance on the class-specific feature f_2 , while simultaneously improving performance. Moreover, it helps mitigate the class imbalance problem.

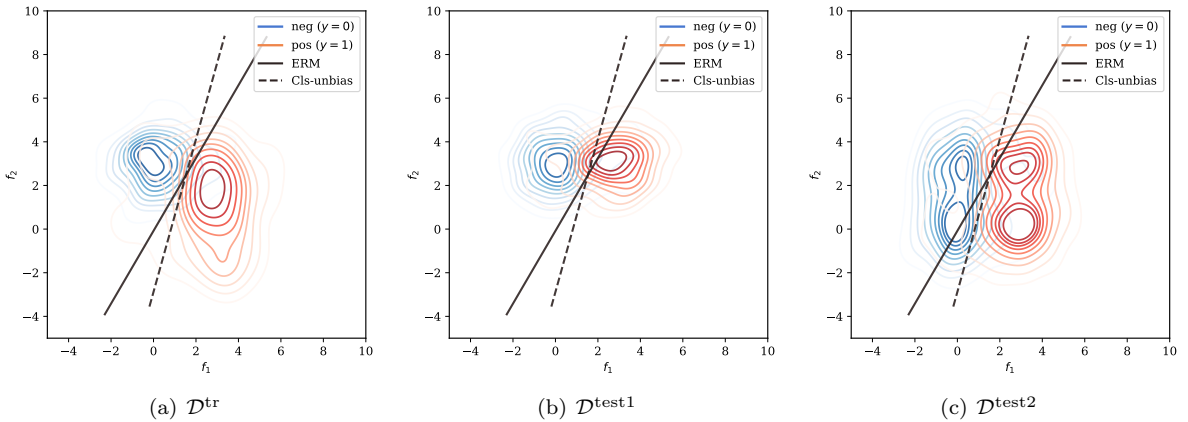


Figure 1: The decision boundaries of a linear classifier trained by the ERM (Eq. 10) and the proposed class-unbiased method (Eq. 9) under the class-balance scenario. The contourplots show distributions of the two features (f_1 and f_2) for the positive (pos) and negative class (neg) for the three datasets: \mathcal{D}^{tr} , $\mathcal{D}^{\text{test1}}$, and $\mathcal{D}^{\text{test2}}$. The positive and negative classes have equal prior in \mathcal{D}^{tr} .

Although simplified, this toy experiment gives an example of class-shared and class-specific features, clearly demonstrates both the existence of the class-feature bias and the effectiveness of our method in addressing it. These findings motivate the application of our approach to more complex, real-world scenarios, as discussed in subsequent sections.

2.2 Class Unbiasing in Real-world Datasets

To evaluate the real-world effectiveness of our class-unbiased method, we tested it on five high-dimensional datasets across speech and medical imaging: two speech-based datasets for depression detection (DAIC-WOZ [26] and MODMA [29]), one for speech-based dementia diagnosis (ADReSS [31]), and two imaging datasets [32]—BreastMNIST for breast cancer detection and a binarized version of RetinaMNIST for diabetic

¹We omit the bias term of the classifier as it does not affect our discussion.

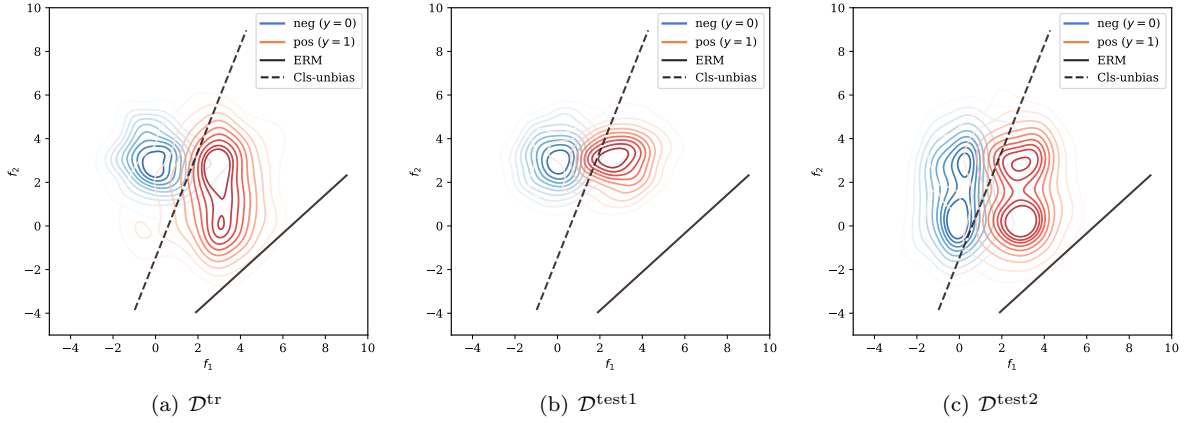


Figure 2: The decision boundaries of a linear classifier trained by the ERM (Eq. 10) and the proposed class-unbiased method (Eq. 9) under the class-imbalance scenario. The contourplots show distributions of the two features (f_1 and f_2) for the positive (pos) and negative class (neg) for the three datasets: \mathcal{D}^{tr} , $\mathcal{D}^{\text{test1}}$, and $\mathcal{D}^{\text{test2}}$. The prior probability of the positive class is 0.1 in \mathcal{D}^{tr} , i.e., $P(y = 1) = 0.1$.

Table 1: Results for the experiments on the synthetic example. For the imbalanced dataset, $P(y = 1) = 0.1$. For meaningful comparisons of the attention to the features f_1 and f_2 by different models, we normalized the model’s weights $\mathbf{w} = [w_1, w_2]$ by $\mathbf{w}/\|\mathbf{w}\|$ and show them in the “Normalized Weights” column.

Row	Method	Class-balanced	Train		Test 1		Test 2		Normalized Weights
			neg-acc	pos-acc	neg-acc	pos-acc	neg-acc	pos-acc	
1	ERM	✓	0.848	0.850	0.880	0.703	0.679	0.825	[0.858, -0.514]
2	Cls-unbias	✓	0.853	0.864	0.876	0.780	0.802	0.845	[0.962, -0.275]
3	ERM	✗	1.000	0.001	1.000	0.000	1.000	0.004	[0.663, -0.749]
4	Cls-unbias	✗	0.852	0.850	0.880	0.708	0.770	0.841	[0.925, -0.379]

retinopathy detection using retinal fundus images. Performance is reported using the macro-averaged F1-score (MF1), which provides a reliable measure under class-imbalanced conditions. The proposed method is compared against two baseline approaches: standard Empirical Risk Minimization (ERM) and class-weighted ERM (ERM (cls-w)).

The main results across five datasets are presented in Table 2. Overall, the proposed class unbiased model consistently outperforms the baselines, across all datasets.

The models trained on most medical datasets suffer from class imbalance, with the issue being particularly severe on DAIC-WOZ where ERM even fails to learn meaningful patterns. While the common class-weighting strategy (ERM (cls-w)) alleviates this problem to some extent, its effectiveness remains limited. In contrast, the class unbiased model outperforms ERM (cls-w), demonstrating its superiority as a solution for class-imbalanced datasets. This improvement stems not only from better handling of class imbalance but also from mitigating potential class-feature bias.

Notably, on the ADRess dataset, where the class distribution is nearly balanced, applying class weighting (ERM (cls-w)) even degrades performance. Meanwhile, the class unbiased model remains effective, suggesting the presence of unseen class-feature bias. This validates the importance of explicitly addressing class-feature bias and underscores the class-unbiased model’s effectiveness in enhancing generalization and robustness, even in class-balanced scenarios.

In addition, we observe that the performance improvements of the class-unbiased model over the baselines are more pronounced on the speech datasets (DAIC-WOZ, MODMA, and ADRess) than the image datasets (BreastMNIST and RetinaMNIST). This is likely because speech tasks are inherently more complex, making it harder for the models to capture true causal relationships, rendering them more susceptible to spurious correlations, including class-feature biases. As a result, the proposed class-unbiased model achieves greater improvements on speech datasets by effectively addressing these potential biases.

2.3 Ablation Study

In medical datasets, class imbalance often results in unreliable modeling of data distributions. The results on the DAIC-WOZ dataset (Table 3) demonstrate a case of severe class imbalance, where the model trained with ERM fails to learn meaningful patterns. Specifically, the model collapses into always predicting the majority

Table 2: Main results on the five real-world datasets. MF1 (with ± 1 standard deviation) for all experiments are reported.

	DAIC-WOZ	MODMA	ADReSS	BreastMNIST	RetinaMNIST
ERM	-	0.714 \pm 0.039	0.493 \pm 0.035	0.814 \pm 0.020	0.647 \pm 0.035
ERM(cls-w)	0.483 \pm 0.048	0.746 \pm 0.027	0.489 \pm 0.031	0.809 \pm 0.023	0.667 \pm 0.032
Cls-unbias	0.627 \pm 0.044	0.782 \pm 0.070	0.530 \pm 0.012	0.833 \pm 0.029	0.682 \pm 0.038

Table 3: Ablation study on DAIC-WOZ.

Row	Method	Valid				Test			
		pos-F1	neg-F1	MF1	Acc	pos-F1	neg-F1	MF1	Acc
1	ERM (per-cls)	0.522 \pm 0.057	0.769 \pm 0.037	0.646 \pm 0.033	0.691 \pm 0.033	0.228 \pm 0.025	0.642 \pm 0.066	0.435 \pm 0.023	0.515 \pm 0.056
2	ERM (cls-w)	0.503 \pm 0.063	0.804 \pm 0.026	0.654 \pm 0.040	0.720 \pm 0.033	0.244 \pm 0.033	0.721 \pm 0.064	0.483 \pm 0.048	0.596 \pm 0.072
3	\mathcal{L}_{g-dro}	0.670 \pm 0.048	0.844 \pm 0.018	0.757 \pm 0.030	0.789 \pm 0.023	0.318 \pm 0.038	0.701 \pm 0.04	0.510 \pm 0.020	0.587 \pm 0.037
4	ERM (per-cls) + $\mathcal{L}_{cls-ineq}$	0.693 \pm 0.035	0.845 \pm 0.008	0.769 \pm 0.019	0.794 \pm 0.011	0.452 \pm 0.048	0.723 \pm 0.027	0.588 \pm 0.025	0.634 \pm 0.025
5	\mathcal{L}_{g-dro} + $\mathcal{L}_{cls-ineq}$	0.717 \pm 0.043	0.858 \pm 0.025	0.788 \pm 0.031	0.811 \pm 0.029	0.510 \pm 0.054	0.744 \pm 0.036	0.627 \pm 0.044	0.664 \pm 0.043

(negative) class, thereby effectively minimizing the cross-entropy loss and achieving around 70% accuracy on the training set. Apparently, this seemingly decent performance is an illusion, as the model fails to detect the minority (positive) class. While the variants of ERM partially alleviate this issue—either through a class-weighting strategy (ERM (cls-w)) or by placing equal emphasis on all classes (ERM (per-cls))—the overall performance remains poor, indicating that the model is still negatively affected by class imbalance and potential class-feature bias.

Class-wise group distributionally robust optimization (\mathcal{L}_{g-dro}) can be used to alleviate the effect of class imbalance, as it adaptively emphasizes the under-explored, underperforming class by assigning higher weight to the minority class. As shown in Table 3, solely using class-wise group distributionally robust optimization (Row 3) is a better approach than using the variants of ERM (ERM (per-cls) & ERM (cls-w)) to handle the class-imbalance problem in the DAIC-WOZ dataset, as the former promotes the exploration of under-represented classes to reduce class loss inequality. However, it fails to handle class-feature bias, because its strategy is to maximize exposure to the minority class rather than minimize reliance on biased class-specific features. In contrast, the class-unbiased models (Rows 4 & 5) substantially improve performance by reducing class loss inequality, thereby mitigating both class imbalance and class-feature bias through explicitly promoting class-wise loss equality, which leads to more generalizable and reliable performance.

Despite the proposed class-inequality loss can reduce class-imbalance, its effectiveness can be negatively affected by severe class-imbalance. This is because the unreliable modeling of class-wise information, caused by class imbalance, can make equalizing class-wise classification losses misleading. Therefore, under scenarios where class imbalance significantly impacts training, we recommend using \mathcal{L}_{g-dro} to obtain a better initial estimate of class-wise information, providing a stronger reference for optimizing the class-inequality loss ($\mathcal{L}_{cls-ineq}$).

Comparing Row 4 and Row 5 of Table 3 further reveals additional improvement brought by incorporating \mathcal{L}_{g-dro} , demonstrating its effectiveness in helping the class-wise inequality loss achieve its intended effect. This is particularly evident on the DAIC-WOZ dataset, where severe class imbalance skews the model’s estimation of class-wise information, thereby limiting the effectiveness of $\mathcal{L}_{cls-ineq}$. By introducing \mathcal{L}_{g-dro} , we mitigate the distortion in the estimated class-wise information caused by class imbalance, improving the overall performance.

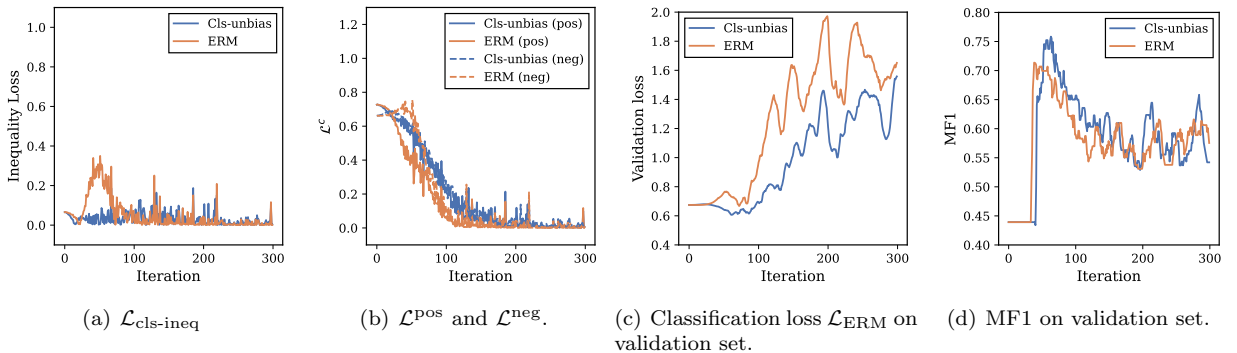


Figure 3: Case study on resampled balanced RetinaMNIST dataset. The number of training samples is 100.

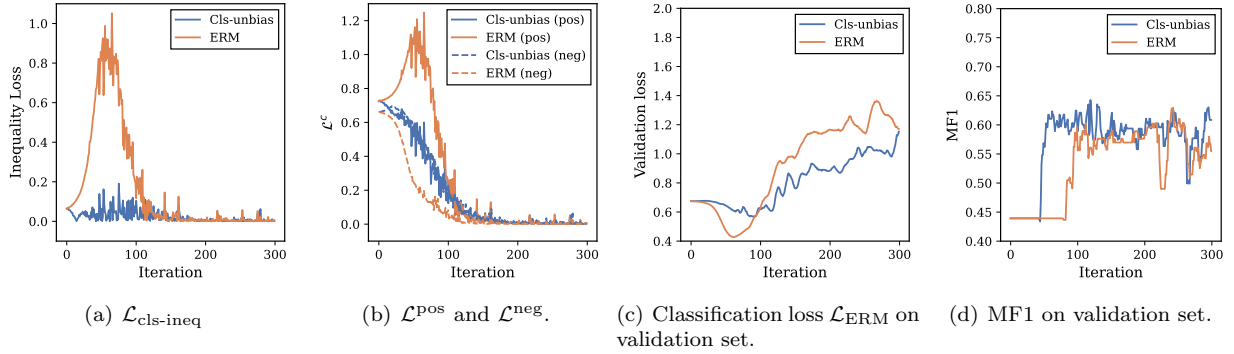


Figure 4: Case study on resampled imbalanced RetinaMNIST dataset. The number of training samples is 100. 25% of training samples are from the positive class.

Table 4: Experimental results on the resampled balanced and imbalanced RetinaMNIST datasets.

Row	Methods	cls-balanced	MF1	Acc
1	ERM	✓	0.621±0.030	0.719±0.041
2	Cls-unbias	✓	0.633±0.023	0.738±0.034
3	ERM	✗	0.568±0.036	0.732±0.026
4	Cls-unbias	✗	0.604±0.039	0.743±0.025

2.4 Case Study on Balanced and Imbalanced Datasets.

To empirically investigate the effect of the proposed class-unbiased approach on balanced and imbalanced datasets, we resampled the RetinaMNIST dataset to construct two settings: a balanced dataset with 100 samples (50% positive) and an imbalanced dataset with 100 samples (25% positive). The experimental results are shown in Table 4. The training processes on both balanced and imbalanced datasets are shown in Figures 3 and 4, respectively.

We first note that the performance improvement of Cls-unbias on the balanced dataset is relatively modest, which is expected since only class-feature bias is addressed in a class-balanced setting. In fact, we found that the degree of inequality varies across different network initializations—some initializations result in substantial inequality. Figure 3 illustrates an initialization that exhibits a significant class loss inequality in the balanced dataset, indicating the presence of class-feature bias. As shown in the figure, reducing this inequality using Cls-unbias leads to lower validation loss (Figure 3(c)) and higher validation MF1 scores (Figure 3(d)). Moreover, the slower increase in validation loss suggests improved generalization and robustness.

In contrast, the effect of Cls-unbias on the imbalanced dataset is much more pronounced (Figure 4), underscoring its effectiveness in addressing both class imbalance and potential class feature bias. Notably, under class imbalance, the severity of class loss inequality is evident, as reflected by the higher values of $\mathcal{L}_{\text{cls-ineq}}$ and a larger gap between \mathcal{L}_{pos} and \mathcal{L}_{neg} compared to the balanced setting under ERM. Specifically, when the model overly focuses on the majority (negative) class, its loss decreases rapidly, while the minority (positive) class loss increases. This results in a lower overall validation loss but comes at the cost of under-representing the minority class and amplifying class loss inequality. Such inequality arises not only from class imbalance but also from class feature bias. Importantly, class feature bias can be exacerbated under class imbalance, as training on imbalanced datasets may encourage the model explore class-specific features, making the role of Cls-unbias even more critical. Overall, the significant improvements observed on the imbalanced dataset highlight the approach’s effectiveness in mitigating both sources of bias.

3 Discussion

In this paper, we identify class-feature bias and highlight it as a significant research problem in medical diagnosis. We proposed a class-wise inequality loss to learn a class-unbiased model that handles class-feature bias and class imbalance simultaneously. For practical considerations, we propose to optimize the model using class-wise G-DRO [5] to enhance the effectiveness of inequality loss under class imbalance. Experimental results shows that the proposed Cls-unbias approach consistently enhances the generalization ability of models under balanced and imbalanced scenarios, across diverse tasks and datasets with different input modalities.

3.1 From Binary Classification to Multi-class Classification

Extending Cls-unbias from binary classification to multi-class classification is feasible. Similar to [24], one possible strategy is to reduce the variance of the class-wise losses. Encouraging class-wise loss equality remains effective when the number of classes is small. Determining the number of classes for which the multi-class extension of Cls-unbias remains valid can be left to future work.

However, as the number of classes increases, the effectiveness of Cls-unbias becomes limited. This is because it is increasingly difficult to identify features that are informative across all classes, as many classes may share many common attributes. Focusing on extracting such class-shared features may result in the model learning few or even no information for prediction, ultimately degrading performance. In such cases, alternative strategies such as matching approaches—for example, comparing extracted feature vectors with learned class prototypes—may be more appropriate. Nevertheless, the proposed definition of class-feature bias provides a useful theoretical foundation for guiding the design of multi-class classification methods, even in settings with a large number of classes.

Finally, we emphasize that Cls-unbias remains highly useful and important in medical diagnosis settings, i.e., binary or few-class classification, where strict feature selection and extraction are critical, as classification failures can lead to severe consequences, including misdiagnosis, delayed treatment, or inadequate monitoring.

3.2 Ethical Impact caused by Class-feature Bias

Class-feature bias, while often subtle and invisible without deliberate awareness, poses significant ethical concerns, especially as deep learning models are increasingly adopted in sensitive domains such as medical diagnosis. This bias arises when the models’ potential reliance on features that are strongly correlated with only a subset of classes, leading to biased performance and poor generalization on other classes. Critically, these “other classes” are more likely to be misclassified, leading not only to increased costs in time and healthcare resources due to misdiagnosis but also to potential ethical harms. For instance, as discussed in the Section 1, using BMI as a dominant predictive feature for diabetes may lead the model to incorrectly associate high BMI with the disease, reinforcing harmful stereotypes and potentially marginalizing individuals with atypical clinical presentations. Such biased representations can exacerbate healthcare disparities and erode trust in AI-assisted medical decisions. Therefore, it is essential to identify and mitigate class-feature bias during model development. Furthermore, this calls for a broader integration of causal learning approaches to ensure more stable, fair, and ethically responsible generalization across diverse patient populations.

4 Method

4.1 Definition of Class-feature Bias

In this section, we formally define class-feature bias as models’ reliance on features that are correlated with only a subset of classes, leading to biased performance and poor generalization on other classes. Mathematically, let the dataset be $\mathcal{D} = \{(\mathbf{x}_i, y_i)\}_{i=1}^N$, where \mathbf{x}_i denotes the input features and $y_i \in \mathcal{C} = \{k\}_{k=0}^{K-1}$ is the class label, with \mathcal{C} the full set of class labels. Assume that some of the K classes can be merged to form one class, resulting in S joint classes. For any subset of classes $\mathcal{C}^s \subseteq \mathcal{C}$, where $s \in \{1, \dots, S\}$, we define the corresponding data subset as $\mathcal{D}^s = \{(\mathbf{x}, y) \in \mathcal{D} \mid y \in \mathcal{C}^s\}$. Then, we have S disjoint subsets $\{\mathcal{D}^s\}_{s=1}^S$ such that $\mathcal{D} = \bigcup_{s=1}^S \mathcal{D}^s$, where \bigcup denotes the union of subsets.

Based on the Bayesian theory, if Y and X are independent, i.e., $P(X, Y) = P(X)P(Y)$, then we have $P(Y|X) = \frac{P(X, Y)}{P(X)} = P(Y)$, where the uppercase letters indicate random variables. Therefore, if there exists a subset \mathcal{D}^m satisfying

$$P(y \in \mathcal{C}^m | \mathbf{x}) = P(y \in \mathcal{C}^m), \text{ for some } m \in \{1, \dots, S\}, \quad (1)$$

and at least one other subset \mathcal{D}^n satisfying

$$P(y \in \mathcal{C}^n | \mathbf{x}) \neq P(y \in \mathcal{C}^n), n \in \{1, \dots, S\} \setminus m, \quad (2)$$

with $P(\cdot)$ denoting the probability, then we say that \mathbf{x} can cause class-feature bias. That is, \mathbf{x} is informative for predicting samples from classes in \mathcal{C}^n , but it is irrelevant to classes in \mathcal{C}^m . Specifically, Eq. 1 indicates that \mathbf{x} carries no information about whether a sample comes from \mathcal{D}^m ; in other words, observing \mathbf{x} does not increase the probability that the sample comes from \mathcal{D}^m .

Class-feature bias has received little attention in the literature. In [25], a special case in multi-class classification of class-feature bias is identified, where \mathcal{C}^n consists of a single class and \mathcal{C}^m includes a subset or all of the remaining classes. However, the authors did not provide a formal or general definition of class-feature bias, and their focus differed from ours. In particular, the authors aimed to keep features of the same class similar

and features of different classes distinct by using a memory queue. However, this approach adds complexity and is less effective on small or low-diversity datasets. In contrast, our method is simple and well-suited for training binary classifiers for medical diagnosis using small medical datasets.

In this study, we first highlight class-feature bias as a significant research problem in medical diagnosis. We focus on binary cases where $\mathcal{C}^m = \{0\}$ and $\mathcal{C}^n = \{1\}$, or alternatively, $\mathcal{C}^m = \{1\}$ and $\mathcal{C}^n = \{0\}$. The Appendix provides a simple example that empirically demonstrates the class-feature bias in the binary case.

4.2 Class-wise Loss Equality

Let $\mathcal{D} = \{\mathcal{D}^{\text{pos}} \cup \mathcal{D}^{\text{neg}}\}$ be a dataset, divided into positive-class and negative-class samples. $P^{\text{pos}}(Y|X)$ and $P^{\text{neg}}(Y|X)$ are the true conditional distributions for samples from the positive and negative classes, respectively. $\hat{P}(Y|X)$ is the predicted conditional distribution from a model, shared for both classes. Our objective is to ensure that the feature X provides a consistent reduction in uncertainty when predicting both positive and negative samples. This consistency indicates that X is informative for distinguishing the samples in the two classes, which can be expressed mathematically as:

$$\mathbb{E}_{\mathcal{D}^{\text{pos}}} H(Y | X) = \mathbb{E}_{\mathcal{D}^{\text{neg}}} H(Y | X), \quad (3)$$

where $\mathbb{E}_{\mathcal{D}^{\text{pos}}} H(Y|X)$ and $\mathbb{E}_{\mathcal{D}^{\text{neg}}} H(Y|X)$ represent the expected conditional entropies for positive and negative samples, respectively.

We express the relationship between the conditional entropy and classification loss as follows:

$$\mathbb{E}_{\mathcal{D}^c} H(Y | X) = \mathcal{L}^c + D_{\text{KL}}(P^c(Y | X) \parallel \hat{P}^c(Y | X)), \quad (4)$$

where $D_{\text{KL}}(P \parallel \hat{P})$ represents the Kullback–Leibler (KL) divergence between distributions P and \hat{P} , $c \in \{\text{pos}, \text{neg}\}$, and \mathcal{L}^c is the cross-entropy loss for samples from \mathcal{D}^c , that is:

$$\mathcal{L}^c = -\mathbb{E}_{\mathcal{D}^c} P^c(Y|X) \log \hat{P}^c(Y|X). \quad (5)$$

Ideally, if the model’s predictions are perfect, i.e., $\hat{P}^c(Y|X) = P^c(Y|X)$, the KL divergence becomes zero, and in that case, when the condition in Eq. 3 is met and $P^c(Y|X)$ is well estimated, we will have

$$\mathcal{L}^{\text{pos}} = \mathcal{L}^{\text{neg}}. \quad (6)$$

In general, the condition in Eq. 6 cannot be met, which is referred to as **class loss inequality**. This inequality can be caused by the following conditions:

1. **Class-feature bias.** The model relies on features X_{spec} that are specific to the class c . In that case, we will have $\mathcal{L}^c < \mathcal{L}^{\neg c}$, where \neg denotes negation. As a result, the model can fail to identify samples from class $\neg c$ in the test set.
2. **Class imbalance.** The model may under-utilize information from X for the minority class c , leading to $\mathcal{L}^c > \mathcal{L}^{\neg c}$.

To address the above problems, we propose to alleviate the inequality between the losses contributed by the positive- and negative-class samples by minimizing a class-wise inequality loss:

$$\mathcal{L}_{\text{cls-ineq}} = |\mathcal{L}^{\text{pos}} - \mathcal{L}^{\text{neg}}|. \quad (7)$$

The minimization of this loss leads to class-unbiased models. The objective $\mathcal{L}_{\text{cls-ineq}}$ is designed to minimize \mathcal{L}_{max} and maximize \mathcal{L}_{min} , where $\mathcal{L}_{\text{max}} = \max(\mathcal{L}_{\text{pos}}, \mathcal{L}_{\text{neg}})$ and $\mathcal{L}_{\text{min}} = \min(\mathcal{L}_{\text{pos}}, \mathcal{L}_{\text{neg}})$. Although maximizing \mathcal{L}_{min} may seem counterintuitive, it serves an important role: it encourages the model to discard class-specific features that are highly informative for one class only (resulting in a low loss) but uninformative for the other class (leading to a high loss).

Intuitively, a large asymmetry or inequality between class-wise classification losses indicates that the model is overfitting to class-specific features, which can harm generalization. By reducing this inequality, the model is guided toward learning features that generalize across classes.

4.3 Group Distributionally Robust Optimization for Class-imbalance

In medical datasets, class imbalance often results in unreliable modeling of data distributions, which leads to difficulties in accurately estimating the posterior probability $P^c(Y|X)$. As discussed in Section 4.2, class imbalance may cause the majority class to dominate in the training process, causing unequal contributions

from the positive and negative classes. The unequal contributions will, in turn, lead to biased and degraded generalization performance in the resulting model.

Specifically, when the inequality between \mathcal{L}^c and \mathcal{L}^{-c} arises due to class imbalance, our objective should be to minimize \mathcal{L}_{\max} , which will in turn minimize the loss of the majority class. However, $\mathcal{L}_{\text{cls-ineq}}$ also encourages maximizing \mathcal{L}_{\min} , which can be counterproductive—particularly under severe class imbalance—by unintentionally penalizing the minority class and destabilizing the optimization. This effect is particularly evident in the early training process, where the minority class receives insufficient attention. To alleviate the detrimental effect of class imbalance, we complement the cross-entropy loss with a G-DRO objective [5], which adaptively emphasizes the under-explored, underperforming class by assigning higher weight to the minority class, mitigating the imbalance and helping the $\mathcal{L}_{\text{cls-ineq}}$ loss work effectively under class-imbalanced situation. Specifically, the G-DRO objective is:

$$\mathcal{L}_{\text{g-dro}} = \sum_{c \in \{\text{pos}, \text{neg}\}} \text{sg} \left(\frac{\exp(\tau \mathcal{L}^c)}{\exp(\tau \mathcal{L}^c) + \exp(\tau \mathcal{L}^{-c})} \right) \mathcal{L}^c, \quad (8)$$

where $\text{sg}(\cdot)$ denotes the stop-gradient operator, i.e., the enclosed term is treated as a constant during backpropagation. Here, τ is a temperature hyper-parameter, which controls the extent to which the model focuses on the worst-performing class (the class with the largest loss). Specifically, when τ is large (e.g., 10), the model places greater emphasis on improving the performance of the worst class; conversely, when τ is small (e.g., 10^{-2}), the model treats both classes more equally. Notably, when $\mathcal{L}^c = \mathcal{L}^{-c}$, the group distributionally robust objective $\mathcal{L}_{\text{g-dro}}$ simplifies to the per-class ERM.

While the class-wise inequality loss $\mathcal{L}_{\text{cls-ineq}}$ can help mitigate the negative effects of class imbalance by minimizing \mathcal{L}_{\max} to some extent, it becomes less effective when the model is already biased. Therefore, under scenarios where class imbalance significantly impacts training, we recommend using $\mathcal{L}_{\text{g-dro}}$ to obtain a better initial estimate of \mathcal{L}_{pos} and \mathcal{L}_{neg} , providing a stronger reference for optimizing $\mathcal{L}_{\text{cls-ineq}}$. Overall, the total loss is defined as:

$$\mathcal{L}_{\text{total}} = \alpha \mathcal{L}_{\text{cls-ineq}} + \mathcal{L}_{\text{g-dro}}. \quad (9)$$

4.4 Baselines: Empirical Risk Minimization

Empirical risk minimization (ERM) has been widely adopted as a fundamental framework for training deep learning models. The goal is to minimize the average loss:

$$\mathcal{L}_{\text{ERM}} = \frac{1}{|\mathcal{B}|} \sum_{(\mathbf{x}, y) \in \mathcal{B}} \ell(\mathbf{x}, y), \quad (10)$$

where \mathcal{B} denotes a batch of data and $\ell(\mathbf{x}, y)$ is the loss (e.g., cross-entropy loss for classification) for the input-target pair (\mathbf{x}, y) .

Variants of ERM, such as class-weighted ERM and per-class ERM, help mitigate the impact of the dominant classes under class-imbalance [6]. In particular, class-weighted ERM modifies the loss function by applying class-dependent scaling factors α_y 's to adjust for class imbalance:

$$\mathcal{L}_{\text{ERM (cls-w)}} = \frac{1}{|\mathcal{B}|} \sum_{(\mathbf{x}, y) \in \mathcal{B}} \alpha_y \ell(\mathbf{x}, y). \quad (11)$$

Per-class ERM computes the loss separately for each class and averages them:

$$\mathcal{L}_{\text{ERM (per-cls)}} = \sum_{c=1}^C \frac{1}{|\mathcal{B}^c|} \sum_{(\mathbf{x}, y) \in \mathcal{B}^c} \ell(\mathbf{x}, y) = \sum_{c=1}^C \mathcal{L}^c, \quad (12)$$

where \mathcal{B}^c denotes the samples in class c in a training batch. Per-class ERM ensures equal emphasis on all classes. Despite these enhancements, challenges remain in balancing performance across diverse distributions and mitigating overfitting in underrepresented classes.

4.5 Related Work on Domain Generalization

The proposed method relates to domain generalization, which aims to improve model robustness under distributional shifts—where the distribution of unseen test data differs from that of the training data. Existing approaches to address the distributional shift mainly fall into two complementary categories: 1) reduce domain discrepancies by making the data representations from different domains similar, using techniques such as data

augmentation [10, 11, 12], feature alignment [13, 14, 15], or gradient matching [16, 17]; and 2) remove domain-specific information/factors, typically through disentanglement [18, 19], invariant risk minimization [20, 21, 22], parameter decomposition [23], or sample reweighting [5]. For example, UndoBias [23] enables support vector machines (SVMs) to handle dataset bias by learning both shared and dataset-specific weights, allowing the SVMs to separate dataset-specific biases from general object features. Invariant risk minimization (IRM) [20, 22] aims to learn predictors that generalize across diverse environments by promoting invariance in the learned representations.

Our study aligns with the second category. Closely related prior work includes Risk Extrapolation (REx) [24] and Group Distributionally Robust Optimization (G-DRO) [5]. Specifically, REx [24] minimizes the variance of training risks to achieve consistent performance across domains, encouraging loss equality at the domain level. In contrast, our work focuses on promoting loss equality at the class level to mitigate class-feature bias, and we establish its theoretical foundation using information-theoretic principles. G-DRO [5], which is designed for optimizing the worst-case group performance, is employed to address the challenges posed by extreme class imbalance.

4.6 Datasets

The proposed method was evaluated on five medical datasets, including three speech datasets and two imaging datasets. Table 5 shows the detailed information about the number of samples in the positive and negative classes in these datasets.

4.6.1 Speech Datasets

DAIC-WOZ. We utilized the Distress Analysis Interview Corpus Wizard-of-Oz (DAIC-WOZ) dataset [26], a widely-used benchmark for depression diagnosis. The dataset comprises clinical interviews from 189 participants, totaling approximately 30 hours of conversation data. Each interview was transcribed and annotated with the participants’ depression status, as determined by the PHQ-8 scale [27]. According to the official division of DAIC-WOZ dataset, we trained the models on the training set, validated on the development set, and tested on the test set. Pretrained wav2vec features [28] were extracted and preprocessed as stated in [3].

MODMA. The Multimodal Open Dataset for Mental Disorder Analysis (MODMA) [29] is a depression dataset collected and released by Lanzhou University from the Second Hospital of Lanzhou University, containing audio recordings from 52 individuals. In MODMA, the positive class constitutes 43% of the data. We followed the splits of training, validation, and test set in [30]. The waveforms were segmented into 3.84-second segments, and 80-dimensional filterbank features (FBanks) were extracted as the model input.

ADReSS. The ADReSS dataset [31] is a speech-based dementia dataset, comprising speech recordings and their transcripts of participants describing the Cookie Theft picture from the Boston Diagnostic Aphasia Exam. The dataset includes 78 dementia participants and 78 healthy controls. Audio recordings were segmented to 3.84s segments, and 80-dimensional FBanks were extracted for training.

4.6.2 Imaging Datasets

The MedMNIST benchmark [32] provides medical imaging datasets designed for the rapid evaluation of machine learning methods on clinical tasks, including breast cancer diagnosis (BreastMNIST), diabetic retinopathy severity prediction (RetinaMNIST), colorectal cancer detection (PathMNIST), among others. We evaluated our method on the BreastMNIST and RetinaMNIST datasets, and we followed the official division of training, validation, and test sets.

BreastMNIST. BreastMNIST contains 780 breast ultrasound images with a resolution of 28×28 pixels. It is designed for binary classification task where breast ultrasound images are categorized into “positive” (normal and benign) and “negative” (malignant).

RetinaMNIST. RetinaMNIST is designed for ordinal regression to predict the severity level of diabetic retinopathy, a diabetes-related eye disease, using retina fundus images. The labels correspond to five ordered levels of severity (0-4). We modified the dataset for binary classification by assigning levels 0 and 1 to the negative class, and levels 2-4 to the positive class.

4.7 Model Structure

4.7.1 Speech Models

The encoders of the speech models for the DAIC-WOZ, MODMA, and ADReSS datasets are three-layer fully connected (FC) networks with a \tanh activation function in their hidden layers. The network structures are $[\text{dim}^{\text{in}}, \text{dim}^{\text{in}} - \frac{\text{dim}^{\text{in}} - \text{dim}^{\text{out}}}{2}, \text{dim}^{\text{out}}]$, where dim^{in} is the dimension of the input features, and dim^{out} denotes the output dimension (12, 16, and 16 for the DAIC-WOZ, MODMA, and ADReSS datasets, respectively). The

Table 5: The number of positive and negative samples in the training and test sets of the five datasets used in this study.

	Train		Test	
	pos	neg	pos	neg
DAIC-WOZ [26]	31	76	14	33
MODMA [29]	9	12	13	14
ADReSS [31]	37	33	22	23
BreastMNIST [32]	399	147	114	42
RetinaMNIST [32]	260	820	88	312

Table 6: Hyper-parameter settings for experiments. lr is learning rate, B is batch size, ω is warm-up ratio, and λ is the hyper-parameter controlling the regularization strength of weight decay.

Dataset	lr	Iterations	B	ω	λ	$\alpha^{\text{init}} \rightarrow \alpha^{\text{end}}$	$\tau^{\text{init}} \rightarrow \tau^{\text{end}}$
DAIC-WOZ [26]	3×10^{-3}	100	-	0.1	0	0→1	2→0.01
MODMA [29]	1×10^{-3}	200	-	0.5	0	0→1	2→0.01
ADReSS [31]	1×10^{-3}	100	-	0.1	0.01	0→1	10→1
BreastMNIST [32]	3×10^{-4}	200	128	0.5	0.01	0→2	10→1
RetinaMNIST [32]	1×10^{-4}	150	64	0.1	0	1→2	10→1

frame-based outputs of the encoders were fed into a statistics pooling layer to obtain segment-level vectors by concatenating the vectors representing the mean across time, the standard deviation across time, and the mean first-order difference between successive feature frames. The pooled vectors were projected to one dimension via a linear layer to output the diagnosis state.

4.7.2 Vision Models

The encoders of the vision models follow the same experimental setting as described in [30]. The classifiers of the vision models are FC layers with dimensions [64, 128, 128, 1], using a ReLU activation function in the hidden layers.

4.8 Evaluation

We primarily focused on the F1-score and accuracy. As both the overall diagnostic accuracy and the model’s performance on individual classes are important, especially in scenarios involving class-feature bias and class imbalance. We used the Macro-averaged F1-score (MF1), the F1-score for the positive class (pos-F1), and the F1-score for the negative class (neg-F1) as our evaluation metrics. Each experiment was repeated five times with different random initializations, and the reported results are the average performance across the five runs.

4.9 Optimization

The values of hyper-parameters are shown in Table 6. The hyper-parameters α and τ were dynamically adjusted during training, changing linearly from α^{init} to α^{end} , and from τ^{init} to τ^{end} , respectively. Specifically, α was increased ($\alpha^{\text{init}} < \alpha^{\text{end}}$) during training to ensure that $\mathcal{L}_{\text{cls-ineq}}$ gradually took effect after $\hat{P}^c(Y|X)$ started to approximate $P^c(Y|X)$, followed by several rounds of model training. On the other hand, τ was decreased ($\tau^{\text{init}} > \tau^{\text{end}}$) to gradually shift the model’s focus from exploring the worst class to treating the two classes equally. This adjustment of τ helps address extreme class imbalance early in the training, preventing failures where $\hat{P}^c(Y|X) \neq P^c(Y|X)$ due to class imbalance, which could degrade the effectiveness of $\mathcal{L}_{\text{cls-ineq}}$.

Cosine learning rate schedules were applied, where the learning rate η was linearly increased from 0 during the initial ω iterations, then it was gradually decreased to 0 according to a cosine curve for the remaining iterations. The Adam optimizer was used for all experiments, with weight decay controlled by λ . For experiments on the speech datasets, each iteration uses samples from one audio segment per unique speaker to ensure balanced speaker representation.

5 Data Availability

The datasets used in this paper are publicly available or available upon request. DAIC-WOZ is available at <https://dcapswoz.ict.usc.edu/>. MODMA is available at <https://modma.lzu.edu.cn/data/index/>. ADReSS is available at <https://talkbank.org/dementia/>. MedMNIST is available at <https://zenodo.org/records/10519652>.

6 Code Availability

Codes for this work are available at <https://github.com/zuo-ls/cls-unbias>. All experiments and implementation details are described in the Methods section.

References

- [1] M Mostafizur Rahman and Darryl N Davis. Addressing the class imbalance problem in medical datasets. *International Journal of Machine Learning and Computing*, 3(2):224, 2013.
- [2] Xingchen Ma, Hongyu Yang, Qiang Chen, Di Huang, and Yunhong Wang. DepAudioNet: An efficient deep model for audio based depression classification. In *Proc. the 6th International Workshop on Audio/Visual Emotion Challenge*, pages 35–42, 2016.
- [3] Lishi Zuo and Man-Wai Mak. Avoiding dominance of speaker features in speech-based depression detection. *Pattern Recognition Letters*, 173:50–55, 2023.
- [4] Mahsa Ghorbani, Anees Kazi, Mahdih Soleymani Baghshah, Hamid R Rabiee, and Nassir Navab. Ragen: Graph convolutional network for disease prediction problems with imbalanced data. *Medical image analysis*, 75:102272, 2022.
- [5] Shiori Sagawa, Pang Wei Koh, Tatsunori B Hashimoto, and Percy Liang. Distributionally robust neural networks. In *International Conference on Learning Representations*.
- [6] Bartosz Krawczyk. Learning from imbalanced data: open challenges and future directions. *Progress in Artificial Intelligence*, 5(4):221–232, 2016.
- [7] Marcus A Badgeley, John R Zech, Luke Oakden-Rayner, Benjamin S Glicksberg, Manway Liu, William Gale, Michael V McConnell, Bethany Percha, Thomas M Snyder, and Joel T Dudley. Deep learning predicts hip fracture using confounding patient and healthcare variables. *NPJ Digital Medicine*, 2, 2019.
- [8] Andrew Bailey and Mark D Plumbley. Gender bias in depression detection using audio features. In *European Signal Processing Conference (EUSIPCO)*, pages 596–600, 2021.
- [9] John R Zech, Marcus A Badgeley, Manway Liu, Anthony B Costa, Joseph J Titano, and Eric Karl Oermann. Variable generalization performance of a deep learning model to detect pneumonia in chest radiographs: a cross-sectional study. *PLoS medicine*, 15(11):e1002683, 2018.
- [10] Shiv Shankar, Vihari Piratla, Soumen Chakrabarti, Siddhartha Chaudhuri, Preethi Jyothi, et al. Generalizing across domains via cross-gradient training. *ICLR*, 2018.
- [11] Riccardo Volpi, Hongseok Namkoong, Ozan Sener, John C Duchi, Vittorio Murino, and Silvio Savarese. Generalizing to unseen domains via adversarial data augmentation. *Advances in Neural Information Processing Systems*, 31, 2018.
- [12] Aayush Prakash, Shaad Boochoon, Mark Brophy, David Acuna, Eric Cameracci, Gavriel State, Omer Shapira, and Stan Birchfield. Structured domain randomization: Bridging the reality gap by context-aware synthetic data. In *International Conference on Robotics and Automation (ICRA)*, pages 7249–7255, 2019.
- [13] Muhammad Ghifary, W Bastiaan Kleijn, Mengjie Zhang, and David Balduzzi. Domain generalization for object recognition with multi-task autoencoders. In *Proceedings of the IEEE International Conference on Computer Vision (ICCV)*, pages 2551–2559, 2015.
- [14] Shanshan Zhao, Mingming Gong, Tongliang Liu, Huan Fu, and Dacheng Tao. Domain generalization via entropy regularization. *Advances in Neural Information Processing Systems*, 33:16096–16107, 2020.
- [15] Rui Gong, Wen Li, Yuhua Chen, and Luc Van Gool. DLOW: Domain flow for adaptation and generalization. In *Proceedings of the IEEE/CVF Conference on Computer Vision and Pattern Recognition*, pages 2477–2486, 2019.
- [16] Yuge Shi, Jeffrey Seely, Philip H. S. Torr, Siddharth Narayanaswamy, Awni Y. Hannun, Nicolas Usunier, and Gabriel Synnaeve. Gradient matching for domain generalization. In *International Conference on Learning Representations (ICLR)*, 2022.

- [17] Alexandre Rame, Corentin Dancette, and Matthieu Cord. Fishr: Invariant gradient variances for out-of-distribution generalization. In *International Conference on Machine Learning*, pages 18347–18377, 2022.
- [18] Divyat Mahajan, Shruti Tople, and Amit Sharma. Domain generalization using causal matching. In *International Conference on Machine Learning (ICML)*, pages 7313–7324, 2021.
- [19] Vihari Piratla, Praneeth Netrapalli, and Sunita Sarawagi. Efficient domain generalization via common-specific low-rank decomposition. In *International Conference on Machine Learning (ICML)*, pages 7728–7738, 2020.
- [20] Martin Arjovsky, Léon Bottou, Ishaan Gulrajani, and David Lopez-Paz. Invariant risk minimization. *arXiv preprint arXiv:1907.02893*, 2019.
- [21] Kartik Ahuja, Ethan Caballero, Dinghuai Zhang, Jean-Christophe Gagnon-Audet, Yoshua Bengio, Ioannis Mitliagkas, and Irina Rish. Invariance principle meets information bottleneck for out-of-distribution generalization. *Advances in Neural Information Processing Systems*, 34:3438–3450, 2021.
- [22] Xiao Zhou, Yong Lin, Weizhong Zhang, and Tong Zhang. Sparse invariant risk minimization. In *International Conference on Machine Learning (ICML)*, pages 27222–27244, 2022.
- [23] Aditya Khosla, Tinghui Zhou, Tomasz Malisiewicz, Alexei A Efros, and Antonio Torralba. Undoing the damage of dataset bias. In *European Conference on Computer Vision (ECCV)*, pages 158–171, 2012.
- [24] David Krueger, Ethan Caballero, Joern-Henrik Jacobsen, Amy Zhang, Jonathan Binas, Dinghuai Zhang, Remi Le Priol, and Aaron Courville. Out-of-distribution generalization via risk extrapolation (rex). In *International Conference on Machine Learning (ICML)*, pages 5815–5826, 2021.
- [25] Qiaowei Miao, Yawei Luo, and Yi Yang. DICS: Find domain-invariant and class-specific features for out-of-distribution generalization. In *IEEE International Conference on Acoustics, Speech and Signal Processing (ICASSP)*, pages 1–5. IEEE, 2025.
- [26] Jonathan Gratch, Ron Artstein, Gale Lucas, Giota Stratou, Stefan Scherer, Angela Nazarian, Rachel Wood, Jill Boberg, David DeVault, Stacy Marsella, David Traum, Skip Rizzo, and Louis-Philippe Morency. The distress analysis interview corpus of human and computer interviews. In *Proc. the 9th International Conference on Language Resources and Evaluation (LREC’14)*, pages 3123–3128, 2014.
- [27] Kurt Kroenke, Tara W Strine, Robert L Spitzer, Janet BW Williams, Joyce T Berry, and Ali H Mokdad. The PHQ-8 as a measure of current depression in the general population. *Journal of Affective Disorders*, 114(1-3):163–173, 2009.
- [28] Steffen Schneider, Alexei Baevski, Ronan Collobert, and Michael Auli. wav2vec: Unsupervised pre-training for speech recognition. In *Proc. Interspeech*, pages 3465–3469, 2019.
- [29] Hanshu Cai, Zhenqin Yuan, Yiwen Gao, Shuting Sun, Na Li, Fuze Tian, Han Xiao, Jianxiu Li, Zhengwu Yang, Xiaowei Li, et al. A multi-modal open dataset for mental-disorder analysis. *Scientific Data*, 9(1):178–187, 2022.
- [30] Lishi Zuo and Man-Wai Mak. Vector quantization-based counterfactual augmentation for speech-based depression detection under data scarcity. *IEEE Journal of Biomedical and Health Informatics*, 2025.
- [31] Saturnino Luz, Fasih Haider, Sofia de la Fuente Garcia, Davida Fromm, and Brian MacWhinney. Alzheimer’s dementia recognition through spontaneous speech, 2021.
- [32] Jiancheng Yang, Rui Shi, Donglai Wei, Zequan Liu, Lin Zhao, Bilian Ke, Hanspeter Pfister, and Bingbing Ni. MedMNIST v2-A large-scale lightweight benchmark for 2d and 3d biomedical image classification. *Scientific Data*, 10(1):41, 2023.